Negative ion properties of trans 2,2′,6,6′-tetrafluoroazobenzene: Experiment and theory

Mohammadreza Rezaee, Yi Wang, Xinxing Zhang, Gaoxiang Liu, Kit Bowen, Andrew M. Bayer, Michel D. Best, and Robert N. Compton

Citation: The Journal of Chemical Physics **143**, 114303 (2015); doi: 10.1063/1.4930599
View online: http://dx.doi.org/10.1063/1.4930599
View Table of Contents: http://scitation.aip.org/content/aip/journal/jcp/143/11?ver=pdfcov
Published by the AIP Publishing

Negative ion properties of *trans* 2,2′,6,6′-tetrafluoroazobenzene: Experiment and theory

Mohammadreza Rezaee,[1] Yi Wang,[2] Xinxing Zhang,[2] Gaoxiang Liu,[2] Kit Bowen,[2] Andrew M. Bayer,[3] Michel D. Best,[3] and Robert N. Compton[1,3]
[1]*Department of Physics, University of Tennessee, Knoxville, Tennessee 37996, USA*
[2]*Departments of Chemistry, John Hopkins University, Baltimore, Maryland 21218, USA*
[3]*Departments of Chemistry, University of Tennessee, Knoxville, Tennessee 37996, USA*

(Received 16 March 2015; accepted 28 August 2015; published online 15 September 2015)

Chemical bonding and the electronic structure of the *trans* 2,2′,6,6′-tetrafluoroazobenzene negative ion have been studied using collision-induced dissociation as well as photodetachment-photoelectron spectroscopy and the experimental results for different properties were compared with the corresponding values calculated using *ab initio* quantum chemistry methods. The *trans* 2,2′,6,6′-tetrafluoroazobenzene anion was prepared by atmospheric pressure chemical ionization for the collision induced dissociation (CID) experiment and through thermal electron attachment in the photodetachment-photoelectron spectroscopy experiments. The adiabatic electron affinity of *trans* 2,2′,6,6′-tetrafluoroazobenzene was measured to be 1.3 ± 0.10 eV using 355 nm, 488 nm, and 532 nm photodetachment photons and the vertical detachment energy was measured to be 1.78 ± 0.10 eV, 2.03 ± 0.10 eV, and 1.93 ± 0.10 eV, respectively. The adiabatic electron affinity was calculated employing different *ab initio* methods giving values in excellent agreement with experimental results. Energy resolved collision induced dissociation experiment study of the precursor anion resulted in 1.92 ± 0.15 eV bond dissociation energy for the collision process yielding $[C_6H_3F_2]^-$ fragment ion at 0 K. Calculations using different *ab initio* methods resulted in a bond dissociation energy ranging from 1.79 to 2.1 eV at 0 K. Two additional CID fragment ions that appear at higher energies, $[C_6H_2F]^-$ and $[C_6H]^-$, are not results of a single bond cleavage. The occurrence of $[C_6H]^-$ is of particular interest since it is the first anion to be observed in the interstellar medium. © *2015 AIP Publishing LLC.* [http://dx.doi.org/10.1063/1.4930599]

I. INTRODUCTION

Azobenzene (diphenyldiazene) consists of two benzene rings connected by single C—N bonds to N═N and exists as *trans* and *cis* isomers exhibiting an orange-red color. First described by the German chemist Mitscherlich[1] in 1834, azobenzene and its derivatives include more than 70% of commercial dyes owing to their vibrant, chemically tunable colors and extreme durability even upon continuous irradiation.[2] Azobenzene and its derivatives are photo-responsive and its *cis*/*trans* geometry can be mechanically changed upon irradiation, making them excellent candidates for photo-switching applications. Photochromic switches that are able to quickly transmit information have attracted a growing interest because of their potential applicability as active data storage and communication elements in many devices, such as optical systems for opto-electronics, holographic materials, and multicolor displays during the last few decades.[3] The *cis* isomer of azobenzene has been known since 1937 when Hartley[4] performed photometric studies of azobenzene and observed that the solubility of azobenzene changed after being irradiated with sunlight. The photo-isomerization can quickly change the geometry of azobenzene from *trans* to the thermodynamically less stable *cis* isomer using UV light (300-400 nm) and the backward reaction occurs using light (visible blue light >400 nm) or thermally on the time scale of minutes.[5]

Azobenzene and its derivatives have attracted much interest because of the large-amplitude structural changes between their *cis* and *trans* isomers, the reversibility of their transformations, and because high photo-stabilities guarantee large numbers of switching cycles.[6] The azobenzene family represents promising candidates for future molecular switches, light harvesting materials, photonic devices, and photo-controllable materials.[7] They also have remarkable biological applications such as the ability to remotely control cellular functions.[8] Designing an azobenzene amino acid opens the possibilities for biological incorporation of photo-switches *in situ*.[9] Azobenzene doped polymers and liquid crystals have fascinating potential applications in biology, photonics, biophysics, and nonlinear optics that have been intensively investigated.[10–12] Fluorinated azobenzene derivatives have been recently synthesized and analyzed. Bushuyev *et al.*[13] studied fluorinated azobenzene and showed that these solids can directly convert visible light into mechanical motion with high isomerization efficiency and chemical stability under multiple isomerization cycles. Functionalizing azobenzene eliminates the need for employing UV light for photo-switching making it more thermally stable and favorable in bio-applications. Recently, Gan *et al.*[14] studied a series of fluorinated azobenzene esters and found that *trans–cis* isomerization occurs after 4 min and *cis–trans* isomerization occurred after 22 h under the same conditions.

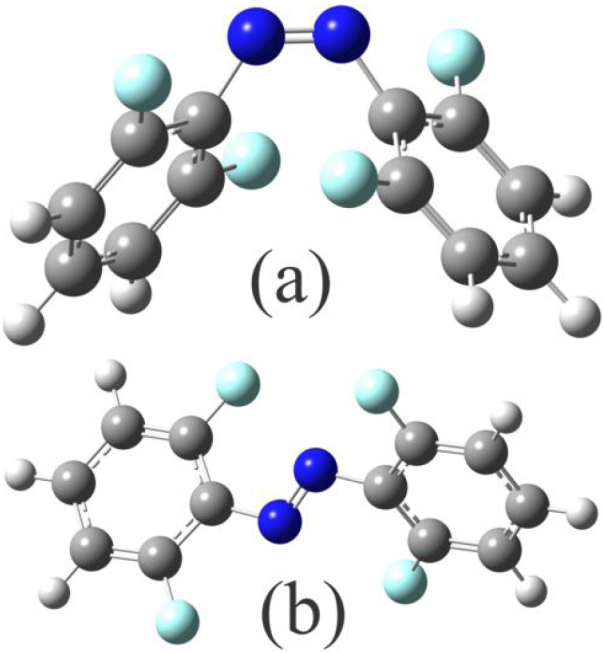

FIG. 1. Optimized structure of 2,2′,6,6′-tetrafluoroazobenzene neutral molecule: (a) *cis* isomer, the CNNC dihedral is −9.2° and the CCNN dihedral angle is 133.2° and (b) *trans* isomer, the CNNC dihedral is −175.9° and the CCNN dihedral angle is 31.2°.

In this research, we studied 2,2′,6,6′-tetrafluoroazo benzene. Figure 1 illustrates the *cis* and *trans* forms of 2,2′,6,6′-tetrafluoroazobenzene optimized at the B3LYP level of theory with 6-311++G(d,p) as the basis set. This calculation results in a 0.29 D dipole moment for the *trans* 2,2′,6,6′-tetrafluoroazobenzene and 5.45 D for the *cis* isomer. Notice that the *trans* isomer is slightly twisted and is not planar, which is the origin of the small dipole moment. *trans* azobenzene is a planar molecule with zero dipole moment. The *trans* 2,2′,6,6′-tetrafluoroazobenzene is 0.36 eV lower in the ground state electronic energy in comparison to the *cis* isomer.

II. EXPERIMENTAL AND COMPUTATIONAL METHODS

A. Synthesis of 2, 2′,6, 6′-tetrafluoroazobenzene

2,6-difluoroaniline (662 μl, 1 g, and 7.745 mmol) was dissolved in 40 ml of dichloromethane. Then, using a mortar and pester, equal weight iron(II) sulphate heptahydrate and potassium permanganate (8 g total) were ground together and added into the flask. The reaction was heated to 40 °C and proceeded as shown (Fig. 2).

The following day the reaction was filtered through Celite and washed with dichloromethane. Column chromatography with 50% dichloromethane in hexanes, then dichloromethane gave product 2,2′,6,6′-tetrafluoroazobenzene (113 mg, 11%). ^{1}H NMR (300 MHz, $CDCl_3$) δ: 7.45-7.28 (m, 2H), 7.13-6.98 (m, 4H). ^{13}C NMR (75 MHz, $CDCl_3$) δ: 157.28 (d, J = 4.1 Hz), 153.82 (d, J = 4.2 Hz), 131.48 (t, J = 10.5 Hz), 112.60 (dd, J = 20.7, 3.4 Hz). 19F (282 MHz, $CDCl_3$) δ: −124.94, referenced to 2,2,2-trifluoroethanol as an external standard. (There is a minor peak due to a small component of the *cis* isomer of the compound, most likely due to exposure to room light.) HRMS-DART: $[M]^-$, calculated for $C_{12}H_6F_4N_2$, 254.0467, found 254.0467.

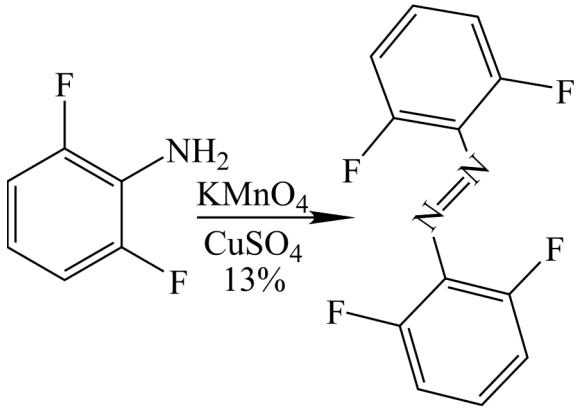

FIG. 2. The reaction scheme for the synthesis of 2,2′,6,6′-tetrafluoro azobenzene.

B. Photodetachment-photoelectron spectroscopy (PD-PES)

Anion photoelectron spectroscopy was conducted by crossing a mass-selected beam of negative ions with a fixed-frequency photon beam and energy-analyzing the resultant photodetached electrons. Photodetachment is governed by the energy-conserving relationship, hν = EBE + EKE, where hν is the photon energy, EBE is electron binding energy, and EKE is electron kinetic energy. Knowing the photon energy and measuring the electron kinetic energy leads to the electron binding energies of the observed transitions.[15] Our anion photoelectron spectrometer, which has been described previously,[16] consists of a laser vaporization anion source, a linear time-of-flight mass analyzer/selector, a pulsed Nd:YAG photodetachment laser (355 nm), and a magnetic bottle electron energy analyzer. Photoelectron spectra were calibrated against the well-known photoelectron spectrum of the copper(I) anion.[17] Parent anions of tetrafluoroazobenzene were generated in a photoemission source. Briefly, tetrafluoroazobenzene sample powder was put into an oven and slightly heated to 30 °C, and the vaporized molecules were then extracted by a plume of helium gas from a pulsed gas valve (backing pressure of ~150 psi). Just outside of the orifice of the oven, low energy electrons were produced by ablating a rotating and translating a Cu rod with a pulsed Nd:YAG laser beam operating at a wavelength of 532 nm. Negatively charged anions were then extracted into the spectrometer prior to mass selection and photodetachment. In addition, PES experiments were carried out using laser photons of 532 nm and 488 nm with identical results to those of 355 nm for the adiabatic electron affinity (AEA).

C. Collision induced dissociation (CID)

CID experiments are well-established quantitative methods based on mass spectrometry to obtain important information about the thermochemical properties of ions. Combined with quantum chemistry computations, CID experiments can be an accurate source of information in gas phase

thermochemistry. Analysis of the cross sections from energy resolved CID experiments can help us to obtain accurate thermodynamic information for a variety of molecular ions.[18,19] The advantage of CID type experiments comparing to the other available quantitative methods is its straightforward procedure for obtaining the bond energies from dissociation cross sections and its versatility to investigate different ions with diverse range of structures.[20] Producing accurate thermodynamic information from CID experiment cross sections requires consideration of many experimental factors that convolute the raw data.[21]

The CID experiments in this work were carried out using an AB SCIEX QSTAR Elite Hybrid LC-MS/MS apparatus consisting of a hybrid quadrupole/time-of-flight mass spectrometer equipped with an atmospheric pressure chemical ionization (APCI) source. A schematic of the QSTAR Elite Hybrid LC/MS/MS and the general method employed has been presented recently by Smith *et al.*[22] in the study of negative ions of *p*-nitroaniline. The *trans* 2,2′,6,6′-tetrafluoroazobenzene sample is first dissolved in methanol as a dilute solution having 2 μg/ml concentration and injected into the instrument with 20 μl/min rate. The gaseous sample is then mixed with nitrogen gas at atmospheric pressure and passed through a short externally heated region. This gas then passes through a ~5 cm tube at room temperature where a corona discharge was used to produce negative ions. Low energy electron attachment to the molecule is followed by collisional stabilization in a bath gas. Atmospheric pressure chemical ionization is suitable for conditions in which electrospray ionization does not work and the compounds which are not highly polar and thermally stable.[23] The ion source temperature is set at 300 °C and the solvent molecules (methanol is a good candidate) initially ionize by the corona discharge. The anions were expanded through a small orifice into the instrument using nitrogen as the curtain gas and through two regions of differential pumping. At the point of entrance into the mass spectrometer, the ions are believed to be at or slightly below room temperature as a result of expansion into the vacuum. The precursor ion of mass m/z = 254 was transmitted through the first quadrupole mass spectrometer (product ion scan) and injected into the collision cell. Argon was used as the neutral collision gas. The collision cell is 20.9 cm long and is at room temperature. The laboratory frame collision energy was varied from 0 eV to 22 eV in increments of 0.10 eV for low collision energy and 0.5 for higher energies and data were recorded for 1 min at each collision energy. We performed the experiment at 22 μTorr and 38 μTorr neutral pressure in the collision cell and the resulting cross sections were linearly extrapolated to zero pressure cross sections. The zero of the kinetic energy scale and the full width at half maximum (FWHM) of the ion kinetic energy distribution are determined by obtaining the derivative of the precursor ion intensity with respect to the energy in the laboratory frame and fitting a Gaussian function to it. The FWHM of ion kinetic energy at the entrance to the collision cell was found to be 0.9 eV. The zero of the energy scale is corrected for 0.27 eV difference between the real and the nominal energy scale and we considered a ±0.05 eV uncertainty in the energy scale based on several measurements and data acquisitions. Analysis of the recorded mass spectrum was performed by using the Analyst® QS 2.0 software provided by the instrument manufacturer company. To convert the data from an instrument dependent ion intensity signal in an energy resolved CID experiment and extract the threshold energy E_0, many factors such as the transition state of the reaction, the non-zero temperature of the neutral target atoms in the collision cell, and the time which it takes for a fragment ion to reach the detector must be considered. Converting the line intensities to cross sections has been performed using the following relationship:[24]

$$I_p = \left(I_p + \Sigma I_f\right) e^{-\sigma_{tot} n \ell}, \tag{1}$$

where I_p is the precursor ion intensity, I_f is the intensity of each fragment ion, σ_{tot} is the total cross section, ℓ is the effective collision cell length, and n is the density of particles in the collision cell, which is related to the pressure and temperature of the neutrals (argon atoms) in the collision cell through $n = P/k_BT$, where P and T in this equation are the collision gas pressure and temperature and k_B is the Boltzmann constant.[25] This is valid provided there are no ions lost in the collision cell or in the path from the collision cell to the detector. There are several uncertainties in this regard. For example, there is an entrance and an exit to the cell which are connected to turbo pumps, resulting in a pressure profile along the collision cell length. Also, if the thin target approximation is valid, i.e., $nl\sigma_{tot} << 1$, then the above equation can be simplified to

$$\sigma_{tot} = \frac{\sum I_f}{nl\left(I_p + \sum I_f\right)}. \tag{2}$$

We used the original form for the sake of accuracy. After calculating the total cross section using relation 1, the cross sections for each of the fragment ions were obtained using

$$\sigma_f = \sigma_{tot}\left(\frac{I_f}{\sum I_f}\right). \tag{3}$$

The conversion from the collision energies in the laboratory frame to the center-of-mass (CM) energy (which is the energy available for deposition into the internal energy of the precursor ion and subsequently will be available for the dissociation reaction to take place) was carried out using the following relation:[26]

$$E_{CM} = E_{lab}\frac{m_{Ar}}{\left(m_{Ar} + m_p\right)}, \tag{4}$$

where m_{Ar} and m_p are the masses of an argon atom and the precursor negative ion, respectively. To obtain the physical threshold energy from the experimental cross section, we utilized the CRUNCH program, which has been developed by the Armentrout group.[17,22–26] Input information for the CRUNCH program includes the number of vibrational degrees of freedom (66), rotational constants and vibrational frequencies for the precursor ion and the transition state of the energized complex, the polarizability of the target argon gas (1.6×10^{-24} cm^3), and the experimental FWHM of the precursor ion kinetic energy distribution. The internal energy of the precursor ion which can contribute to the dissociation reaction and lower the measured threshold, rotational constants, and the vibrational frequencies which are required for the CRUNCH program analysis was obtained from *ab initio* calculations which

were performed using Gaussian 09[27] quantum chemistry package.[28,29] The threshold energy for the dissociation reaction obtained from CRUNCH analysis is for the ground electronic and rovibrational state of the reactant ion at 0 K and CRUNCH program performs summation over the rovibrational states of the reactant ions.[30] The CRUNCH program considers the kinetic shift: the shift of the dissociation energy to higher energies due to the lifetime of the transient intermediates comparable to the time it takes ions to reach the detector from the dissociation region (which in theory should be only the collision cell) by using the RRKM[31–33] (Rice–Ramsperger–Kassel–Marcus) statistical theory to calculate the dissociation rate as a function of the ion internal energy.[34] For a large ion like the sample we studied (with 66 vibrational degrees of freedom), the kinetic shift may be bigger than 1 eV and it is necessary to be considered in the threshold CID measurement analysis.[35] To estimate the uncertainty in the threshold energy measurement, several threshold values were determined from different data sets with variations in the adjustable fit parameter n and also the uncertainty of the absolute energy scale was taken into account, the process suggested by Armentrout to estimate the overall uncertainty in the measured bond energy.[29,36–38]

D. *Ab initio* computations

Quantum mechanical methods, especially *ab initio* approaches, have been widely used for computational thermochemistry and predicting physical and chemical properties of molecules and ions. The field of computational thermochemistry has matured to the point that for small molecules it is possible to predict reaction enthalpies to accuracies rivalling that obtained from the best experiments.[39] Here, we used several hybrid density functional methods as well as high accuracy multi-level calculation, CBS-QB3,[40–42] G3,[43,44] and G4 which is the fourth in the Gaussian-n series[45] to compute the bond dissociation energies (BDEs) along with other properties such as the AEA, the vertical electron affinity (VEA), and the vertical detachment energy (VDE). G4 method which consists of 8 levels of calculation including geometry optimization and frequency calculations using the B3LYP level of theory along with a 6-31G(2df,p) basis set was one of the high level methods utilized in a search to obtain accurate results for the affinities and bond dissociation energies. In the study carried out by Curtiss *et al.* for 63 compounds, the G4 calculated electron affinities showed deviation from experimental results by more than 0.087 eV for only a few compounds.[45] In general, Gaussian-n methods are accurate for calculating molecular energies. CBS-QB3 includes geometry optimization and frequency calculations (which also yields the zero point energy) using B3LYP level of theory and 6-311++G(2d,d,p) Pople basis set and 3 levels of energy calculations. The accurate results from these multi-level methods are highly desirable for properties such as the electron affinity which is very sensitive to the method as well as basis set.

The adiabatic electron affinity is the difference between total energy of the neutral and anion of the molecule in their ground state. The VDE is the energy difference between the neutral at the same geometry of the ground state of the anion and the ground state of the anion. VEA is the energy difference between the ground state of the neutral molecule and the anion at the same geometry as the neutral ground state. Ground state properties of the negative ions and the neutral precursor molecule geometry optimizations along with vibrational frequency calculations were performed using Gaussian 09 quantum chemistry package. All of the molecular structures were initially optimized using the hybrid density functional method, B3LYP, and the tight convergence criteria for optimization and the self-consistent field, SCF, were applied. Care was taken to be certain in the case of a transition state that there was only one negative frequency present in the resulting calculations. For better accuracy of the calculated values, the integrations have been performed with ultrafine grid size (Int = UltraFine). The zero point energy for each method has been calculated from the frequency calculations using a harmonic approximation and it has been scaled with the proper scaling factor, which are mostly obtained from Alecu *et al.*[46] before being added to the total ground-state electronic energy. For cases in which we could not find the exact value for scaling factor for a particular method/basis set, we applied the closest available scaling factor. A transition state search was performed using both the Berny algorithm and the QST3 approach using the STQN (Synchronous Transit-Guided Quasi-Newton) method developed by Schlegel and Peng,[47] which were found to yield almost identical results. Also a loose transition state located at the centrifugal barrier assumption was employed in CRUNCH program analysis.[48] *Ab initio* computations proved that the bond dissociation reaction resulting in 113 m/z fragment ion has no barrier and it is a simple direct bond cleavage (no activation barrier for the reverse reaction).

III. RESULTS AND DISCUSSION

A. Electron affinity measurement experiment

The resultant photoelectron spectrum taken using 488 nm, 532 nm, and 355 nm photodetachment laser photons is presented in Figure 3. One can observe that the first EBE band starts from around 1.1 eV and peaks at 1.78 eV. If there is sufficient Franck-Condon overlap between these two states, the threshold of the first EBE band should be the AEA. However, depending on the anion and the source by which it was generated, it is not uncommon for some degree of vibrational hot band contribution to be present. Taking this possibility into account, we extrapolated the left side of the first EBE band to zero, with the corresponding EBE value there being taken as the AEA. Here, we report the experimental AEA value to be 1.3 ± 0.10 eV obtained from all three photodetachment wavelengths. The measured VDE is slightly different for the three wavelengths: 2.03 eV ± 0.10 for 488 nm, 1.93 eV for 532 nm, and 1.78 ± 0.10 eV for 355 ± 0.10 nm. This could indicate a small difference in Franck-Condon factors for the transitions or the participation of an excited anion at the photon energies involved.

B. Collision induced dissociation experiment

Figure 4 shows the total as well as relative (for the fragment ions) cross sections linearly extrapolated to zero pressure

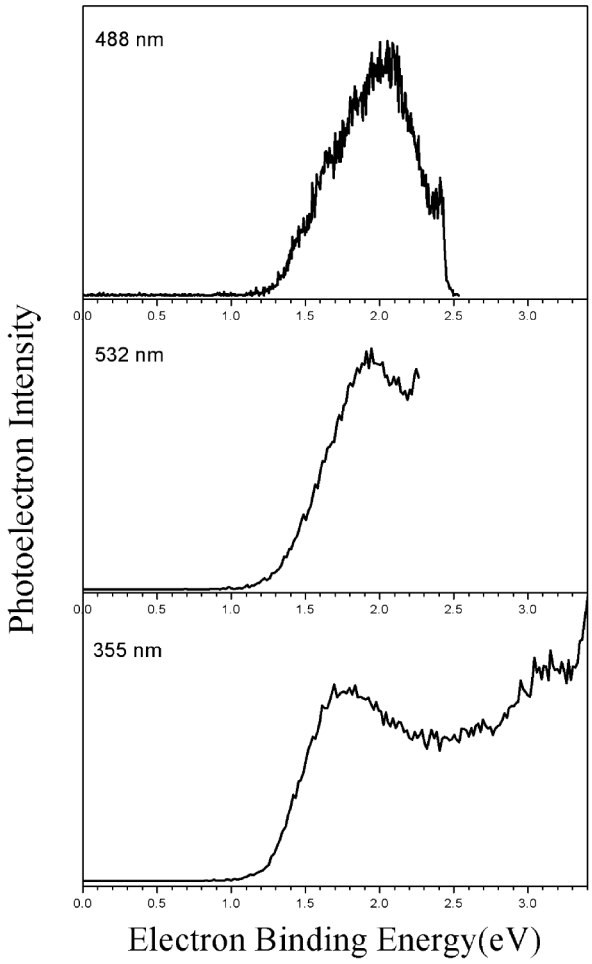

FIG. 3. The photoelectron spectrum of the *trans* 2,2′,6,6′-tetrafluoroazo benzene anion recorded using 488 nm, 532 nm, and 355 nm laser photons.

as a function of collision energy in the center of mass (lower x-axis) and the laboratory frame (upper x-axis). In the low energy region, the predominant fragment ion is 113 m/z, $[C_6H_3F_2]^-$. At the higher energy region peaks that are assigned to the 93 m/z and 73 m/z ions, $[C_6H_2F]^-$ and $[C_6H]^-$, respectively, appear and their intensities grow with increasing the collision energy which are believed to be the result of sequential loss of HF. The maximum cross section for the $[C_6H]^-$ fragment ion is 65.69×10^{-20} m^2, negligible compared to the primary fragment ion cross section 81.06×10^{-18} m^2.

The suggested mechanism to form the three negative fragment ions detected in the mass spectrum can be summarized as

$$[C_{12}H_6F_4N_2]^- + Ar \rightarrow [C_6H_3F_2]^- + [C_6H_3F_2N_2] + Ar \quad (5)$$

$$\rightarrow [C_6H_2F]^- + [HF + C_6H_3F_2N_2] + Ar \quad (6)$$

$$\rightarrow [C_6H]^- + [2HF + C_6H_3F_2N_2] + Ar. \quad (7)$$

The energy dependence of the ion peak intensities was initially analyzed using Analyst software and then converted into a relative cross section by utilizing relation (3). For reactions (6) and (7) (and also the $C_6H_3F_2N_2$ structure in reaction (5)), the brackets indicate that the compositions of the neutral products are unknown. Our theoretical calculations which were performed at the B3LYP level of theory using 6-311++G(d,p) basis set proved the $C_6H_3F_2N_2$ structure is 0.33 eV higher in the ground state energy compared to the $C_6H_3F_2 + N_2$ which suggests after the first C—N bond dissociation, the second C—N bond dissociation will carry on spontaneously.

In CRUNCH analysis, we followed the theory for the transition state of the dissociation developed by Rodgers, Ervin, and Armentrout that models reaction by loosely interacting products such that both fragments are free to rotate (loose transition state or the phase space limit).[18,49–51] Figure 5 shows

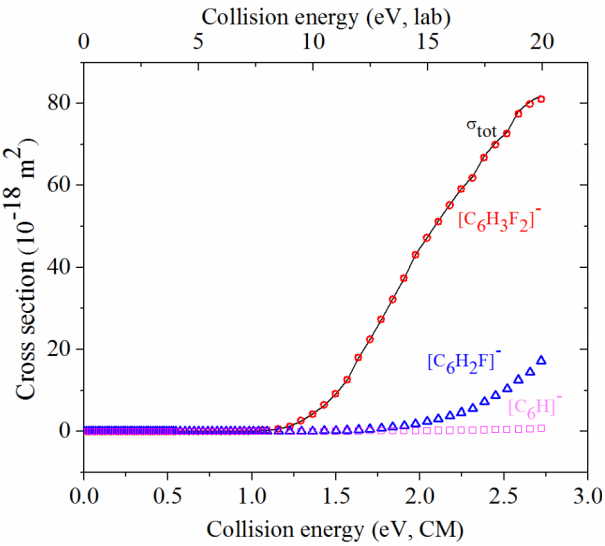

FIG. 4. Zero pressure extrapolated cross sections for the dissociation reaction of 2,2′,6,6′-tetrafluoroazobenzene anion with argon as a function of collision energy in the center of mass (CM) and the laboratory frame. The solid black line is the absolute (total) cross section and as we can see it overlaps for most of the collision energies with the cross section for the 113 m/z fragment ion since it is the only predominant fragment ion.

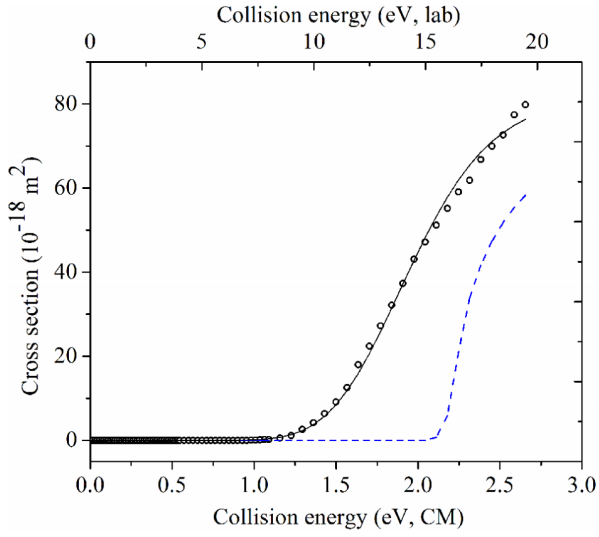

FIG. 5. Zero pressure extrapolated experimental collision-induced dissociation cross section for the bond cleavage reaction with argon yielding the m/z = 113 fragment ion as a function of collision energy in CM and laboratory frame. Solid line is the CRUNCH fit to the cross section. The dashed line which is the result of CRUNCH program analysis is the deconvoluted cross section when the broadening effects of experimental kinetic energy and the internal energy are corrected for 0 K.

the fit of the experimental cross section with an empirical model[52–55] generated by the CRUNCH program along with the deconvoluted cross section. The dashed line shows the model cross section when there is no kinetic energy broadening and the reactant ions are at 0 K with ground state electronic, vibrational, and rotational internal energy.[36] This procedure yields 1.92 eV for the threshold bond dissociation energy. Considering all the uncertainties and the scheme explained before, we determined ±0.15 eV for the overall uncertainty in bond dissociation energy.

The $[C_6H]^-$ which appeared in the CID mass spectrum at laboratory energies above 20 eV at 22 μTorr neutral pressure in collision cell is a specifically interesting anion since it and the other C_nH^- anions represent the first negative ions observed in the interstellar medium. McCarthy *et al.*[56] described the detection of $[C_6H]^-$ in the radio band in the laboratory, which has been identified in the molecular envelope of IRC + 10 216 and in the dense molecular cloud TMC-1. The cross section for this fragment ion is negligible in comparison to the main fragment ion. Since the two other fragment ions are not the results of simple one bond dissociation, no attempt had been made to perform the analysis on the cross sections related to those fragments.

C. Quantum chemical computations

Table I summarizes the calculated BDE, cleaving the C—N bond, for the *trans* 2,2′,6,6′-tetrafluoroazobenzene anion at 0 K. The experimental result obtained from CRUNCH program analysis is for this temperature as well. Comparing the result from threshold collision induced dissociation experiment, we can see the G4 and CBS-QB3 perform well in predicting the BDE where the G3 theory yields results 0.18 eV different from the experimentally measured value. Comparing the experimentally measured BDE with several hybrid density functional methods' results, we can see the performance of those in calculating bond dissociation energy for the studied anion. Comparing the results from several different density functional methods, wB97[57,58] method family performs exceptionally well and the results are comparable to the ones from multi-level calculations. Both G4 and wB97 methods resulted in BDE with 9.97×10^{-3} eV absolute deviation from the experiment. In addition, the results from different basis set sizes, with B3LYP method we can see that the aug-cc-pVDZ Dunning basis set has a better performance in predicting the BDE. The M06 and M06-L methods overestimate the BDE by ~0.2 eV, while the B3LYP results are smaller than the experimental result. M06-2X result for the BDE has ~0.087 eV deviation from the experimental value, better result comparing with the M06-L method by a factor of two.

TABLE I. Calculated Bond Dissociation Energies (BDEs) at 0 K for cleaving the C—N bond of the precursor ion yielding the $[C_6H_3F_2]^-$ anion and $C_6H_3F_2N_2$ neutral fragment.

Method/basis set	Bond dissociation energy (eV)
B3LYP/6-31+G(d)	1.84
B3LYP/6-311+G(d)	1.79
B3LYP/6-311++G(d)	1.79
B3LYP/6-311++G(d, p)	1.79
B3LYP/6-311++G(2d, 2p)	1.80
B3LYP/6-311++G(3df, 3pd)	1.83
B3LYP/aug-cc-pVDZ	1.86
M06/6-311++G(d, p)	2.08
M06-L/6-311++G(d, p)	2.10
M06-2X/6-311++G(d, p)	2.01
B3P86/6-311++G(d, p)	1.97
B3PW91/6-311++G(d, p)	1.88
wB97/6-311++G(d, p)	1.91
wB97X/6-311++G(d, p)	1.90
wB97XD/6-311++G(d, p)	1.95
CBS-QB3	1.90
G3	2.10
G4	1.93
Experiment	1.92 ± 0.15

Taking into account the estimated experimental uncertainty, most of the calculations are compatible with the experimental result. BDEs calculated using the B3LYP method are lower than the experimental value regardless of the basis set size. Overall, the average absolute deviation from the experimental value for the BDE from all of the performed calculations is less than 0.087 eV.

Table II presents the computational results for the vertical detachment energy, adiabatic electron affinity, and the vertical electron affinity for the trans 2,2′,6,6′-tetrafluoroazobenzene at 298.15 K since this is a good approximation for the temperate in which the experimental measurement of the electron affinities was performed. The method used to calculate the adiabatic and vertical molecular electron affinities and also the vertical detachment energy was explained in detail by Rienstra-Kiracofe *et al.* before.[59] In these results for the electron affinities, we always included the zero point vibrational energies in the calculations. One of the interesting results from comparing these calculations with the experimentally measured value for the adiabatic electron affinity is the exceptionally good performance of G3 theory. The highly accurate multi-level method, G3, gives a value of 1.28 eV at 298.15 K which is in excellent agreement with the experimental value for the adiabatic electron affinity. Deviation from experimental value using G3MP2 theory is not small (0.12 eV) comparing to G3 theory performance. None of the hybrid density functional methods used is better than ~0.3 eV deviation from the experientially measured adiabatic electron affinity. Summary of the deviations of the results from different *ab initio* calculations for the adiabatic electron affinity (experimental value – theoretical value) from the experimental value for the *trans* 2,2′,6,6′-tetrafluoroazobenzene which gives a good insight about the performance of these different theories is also provided in eV unit. B3LYP deviation basis set size dependence for the adiabatic electron affinity is not systematic. Overall we can conclude that G3, CBS-QB3, and G3MP2 had the best performance in predicating the adiabatic electron affinity for the *trans* 2,2′,6,6′-tetrafluoroazobenzene and the deviation of the G4 result is twice as big as the CBS-QB3 result. The multi-level high accuracy methods always perform an initial geometry optimization procedure and since calculating VDE or VEA requires keeping the geometry of the neutral at optimized

TABLE II. Summary of the calculated vertical detachment energy (VDE), adiabatic electron affinity (AEA), vertical electron affinity (VEA) in eV unit, and the dipole moment (in D) for the *trans* 2,2′,6,6′-tetrafluoroazobenzene at 298.15 K. Scale factor is for the zero point energy scaling. Deviations of the adiabatic electron affinity resulted from different theoretical methods compared to the experimental value in eV unit.

Method/basis set	VEA	AEA	VDE	Scale factor	Neutral dipole moment	Anion dipole moment	Deviation
B3LYP/6-31+G(d)	1.25	1.70	1.75	0.98	0.27	0.3	−0.39
B3LYP/6-311+G(d)	1.27	1.74	1.80	0.98	0.29	0.34	−0.44
B3LYP/6-311++G(d)	1.27	1.75	1.80	0.98	0.26	0.00	−0.45
B3LYP/6-311++G(d, p)	1.28	1.76	1.82	0.98	0.29	0.35	−0.46
B3LYP/6-311++G(2d, 2p)	1.24	1.71	1.77	0.98	0.27	0.00	−0.41
B3LYP/6-311++G(3df, 3pd)	1.24	1.70	1.76	0.981	0.26	0.00	−0.40
B3LYP/aug-cc-pVDZ	1.30	1.73	1.79	0.98	0.24	0.00	−0.42
M06/6-311++G(d, p)	1.85	2.30	2.36	0.971	0.25	0.38	−1.00
M06L/6-311++G(d, p)	1.28	1.75	1.80	0.972	0.34	0.45	−0.45
M062X/6-311++G(d, p)	1.27	1.75	1.84	0.98	0.20	0.00	−0.45
wB97/6-311++G(d, p)	1.24	1.65	1.68	0.978	0.20	0.00	−0.35
wB97X/6-311++G(d, p)	1.10	1.66	1.80	0.967	0.22	0.00	−0.36
wB97XD/6-311++G(d, p)	0.91	1.62	1.81	0.971	0.26	0.00	−0.31
B3PW91/6-311++G(d, p)	0.95	1.62	1.78	0.971	0.30	0.34	−0.31
B3P86/6-311++G(d, p)	1.00	1.62	1.74	0.975	0.29	0.29	−0.32
CBS-QB3		1.41			0.20	0.00	−0.11
G3		1.28					0.02
G3MP2		1.18					0.12
G4		1.54					−0.24
Experimental		1.3 ± 0.10	1.78 ± 0.10[a]				

[a]This experimental result obtained by using 355 nm laser wavelength.

anion structure and anion at the neutral optimized structure, respectively, intact, we did not calculate the VDE or VEA using those methods.

Finally, we note that our initial experimental studies of this molecule were focused on an attempt to observe a difference in the anion properties of the *trans* and *cis* isomers. It was possible to use a green light-emitting diode (LED) light source to produce a sample of 2,2′,6,6′-tetrafluoroazobenzene solution in chloroform-d with >90% *cis* composition based upon NMR analysis. However, due to the high temperature (300 °C) of the ion source, we were not able to measure the threshold for the bond dissociation energy of the *cis* isomer, expected to be ~0.36 eV lower than the correspondence BDE for the *trans* isomer. Since the *cis* isomer is thermodynamically less stable, it converts to *trans* isomer upon heating. For completeness, the electron affinity and the vertical detachment energy of the *cis* isomer were calculated as well. Table III is a comparison of the calculated results for the VDE, AEA, and VEA for the *cis* and *trans* isomers using the B3LYP level of theory along with 6-311++G(2d,2p) Pople basis set.

TABLE III. Vertical detachment energy (VDE), adiabatic electron affinity (AEA), and vertical electron affinity (VEA) for the *cis* and *trans* isomers of 2,2′,6,6′-tetrafluoroazobenzene. Energies are in eV unit and dipole moment is in D.

Isomer	VDE	AEA	VEA	Dipole moment
cis	1.94	1.47	0.99	5.18
trans	1.77	1.63	1.24	0.27

IV. CONCLUSION

Collision induced dissociation and photodetachment-photoelectron spectroscopy have been employed to study the *trans* 2,2′,6,6′-tetrafluoroazobenzene anion and the results were compared with those obtained from different *ab initio* calculations. Photoelectron spectroscopy provided an adiabatic electron affinity of 1.3 ± 0.10 eV using 355, 532, and 488 nm laser photons and a vertical detachment energy of 1.78 ± 0.1 eV, 2.03 ± 0.1 eV, and 1.93 ± 0.1 eV, respectively. Gaussian-3 theory performs very well for the electron affinities' prediction. Collision induced dissociation of the precursor anion $[C_{12}H_6N_2F_4]^-$ yields the fragment ion $[C_6H_3F_2]^-$, i.e., breakage of a C—N bond. The calculated values for the BDE for the CN bond cleavage using different levels of theory and basis sets at 0 K were compared with the experimentally obtained value from the collision induced dissociation threshold measurement, 1.92 ± 0.15 eV. The Gaussian-4 theory, CBS-QB3, and wB97XD quantum chemical calculations provided results for the BDE in excellent agreement with the experimental value.

ACKNOWLEDGMENTS

We are thankful to Dr. Peter B. Armentrout for providing the CRUNCH program and utilizing it along with many helpful discussions and comments. We are also grateful to Dr. John E. Bartmess for his technical assistance and useful comments. We are also thankful to NEWTON high performance computing program, University of Tennessee, Knoxville, for the generous computation time.

This material is based in part on work supported by the National Science Foundation under Grant No. CHE-1360692 (K.H.B.).

[1]E. Mitscherlich, Ann. Pharm. **9**, 39–48 (1834).
[2]T. A. Singleton, K. S. Ramsay, M. M. Barsan, I. S. Butler, and C. J. Barrett, J. Phys. Chem. B **116**, 9860–9865 (2012).
[3]J. Garcia-Amoros and D. Velasco, Beilstein J. Org. Chem. **8**, 1003–1017 (2012).
[4]G. Hartley, Nature **140**, 281 (1937).
[5]S. Samanta, T. M. McCormick, S. K. Schmidt, D. S. Seferos, and G. A. Woolley, Chem. Commun. **49**, 10314–10316 (2013).
[6]R. Siewertsen, H. Neumann, B. Buchheim-Stehn, R. Herges, C. Nather, F. Renth, and F. Temps, J. Am. Chem. Soc. **131**, 15594–15595 (2009).
[7]A. Emoto, E. Uchida, and T. Fukuda, Polymers **4**, 150–186 (2012).
[8]S. Sawada, N. Kato, and K. Kaihatsu, Curr. Pharm. Biotechnol. **13**, 2642–2648 (2012).
[9]A. Goulet-Hanssens and C. J. Barrett, J. Polym. Sci., Part A: Polym. Chem. **51**, 3058–3070 (2013).
[10]Z. Mahimwalla, K. G. Yager, J.-i. Mamiya, A. Shishido, A. Priimagi, and C. J. Barrett, Polym. Bull. **69**, 967–1006 (2012).
[11]L. Rocha, C.-M. Păiuş, A. Luca-Raicu, E. Resmerita, A. Rusu, I.-A. Moleavin, M. Hamel, N. Branza-Nichita, and N. Hurduc, J. Photochem. Photobiol., A **291**, 16–25 (2014).
[12]S. K. Yesodha, C. K. S. Pillai, and N. Tsutsumi, Prog. Polym. Sci. **29**, 45–74 (2004).
[13]O. S. Bushuyev, A. Tomberg, T. Friščić, and C. J. Barrett, J. Am. Chem. Soc. **135**, 12556–12559 (2013).
[14]S. Gan, A. Yuvaraj, M. Lutfor, M. Mashitah, and H. Gurumurthy, RSC Adv. **5**, 6279–6285 (2015).
[15]S. Eustis, D. Wang, S. Lyapustina, and K. H. Bowen, J. Chem. Phys. **127**(22), 224309 (2007).
[16]X. Zhang, Y. Wang, H. Wang, A. Lim, G. Gantefoer, K. H. Bowen, J. U. Reveles, and S. N. Khanna, J. Am. Chem. Soc. **135**, 4856–4861 (2013).
[17]J. Ho, K. M. Ervin, and W. C. Lineberger, J. Chem. Phys. **93**, 6987–7002 (1990).
[18]M. T. Rodgers, K. M. Ervin, and P. B. Armentrout, J. Chem. Phys. **106**(11), 4499–4508 (1997).
[19]M. T. Rodgers and P. B. Armentrout, J. Chem. Phys. **109**(5), 1787–1800 (1998).
[20]F. Muntean and P. B. Armentrout, J. Chem. Phys. **115**(3), 1213–1228 (2001).
[21]A. F. Sweeney and P. B. Armentrout, J. Chem. Phys. A **118**(44), 10210–10222 (2014).
[22]B. H. Smith, A. Buonaugurio, J. Chen, E. Collins, K. H. Bowen, R. N. Compton, and T. Sommerfeld, J. Chem. Phys. **138**(23), 234304 (2013).
[23]A. Bruins, TrAC, Trends Anal. Chem. **13**(2), 81–90 (1994).
[24]P. B. Armentrout, J. Am. Soc. Mass Spectrom. **13**(5), 419–434 (2002).
[25]P. B. Armentrout, J. Anal. At. Spectrom. **19**(5), 571–580 (2004).
[26]J. Appell and R. Cooks, in *Collision Spectroscopy*, edited by R. G. Cooks (Plenum, New York, 1978), p. 227.
[27]M. J. Frisch, G. W. Trucks, H. B. Schlegel, G. E. Scuseria, M. A. Robb, J. R. Cheeseman, G. Scalmani, V. Barone, B. Mennucci, G. A. Petersson, H. Nakatsuji, M. Caricato, X. Li, H. P. Hratchian, A. F. Izmaylov, J. Bloino, G. Zheng, J. L. Sonnenberg, M. Hada, M. Ehara, K. Toyota, R. Fukuda, J. Hasegawa, M. Ishida, T. Nakajima, Y. Honda, O. Kitao, H. Nakai, T. Vreven, J. A. Montgomery, Jr., J. E. Peralta, F. Ogliaro, M. Bearpark, J. J. Heyd, E. Brothers, K. N. Kudin, V. N. Staroverov, R. Kobayashi, J. Normand, K. Raghavachari, A. Rendell, J. C. Burant, S. S. Iyengar, J. Tomasi, M. Cossi, N. Rega, J. M. Millam, M. Klene, J. E. Knox, J. B. Cross, V. Bakken, C. Adamo, J. Jaramillo, R. Gomperts, R. E. Stratmann, O. Yazyev, A. J. Austin, R. Cammi, C. Pomelli, J. W. Ochterski, R. L. Martin, K. Morokuma, V. G. Zakrzewski, G. A. Voth, P. Salvador, J. J. Dannenberg, S. Dapprich, A. D. Daniels, Ö. Farkas, J. B. Foresman, J. V. Ortiz, J. Cioslowski, and D. J. Fox, GAUSSIAN 09, Revision D.01, Gaussian, Inc., Wallingford, CT, 2009.
[28]M. T. Rodgers and P. B. Armentrout, Acc. Chem. Res. **37**(12), 989–998 (2004).
[29]T. E. Cooper and P. B. Armentrout, J. Chem. Phys. **134**(11), 114308 (2011).
[30]P. B. Armentrout, B. Yang, and M. T. Rodgers, J. Phys. Chem. B **117**(14), 3771–3781 (2013).
[31]P. J. Robinson and K. A. Holbrook, *Unimolecular Reactions* (Wiley-Interscience, New York, 1972).
[32]T. Baercor and P. M. Mayerfn, J. Am. Soc. Mass Spectrom. **8**(2), 103–115 (1997).
[33]W. Forst, *Theory of Unimolecular Reactions* (Elsevier, 2012).
[34]P. B. Armentrout, Int. J. Mass Spectrom. **227**(3), 289–302 (2003).
[35]K. Vékey, J. Mass Spectrom. **31**(5), 445–463 (1996).
[36]P. B. Armentrout, B. Yang, and M. T. Rodgers, J. Phys. Chem. B **118**(16), 4300–4314 (2014).
[37]C. A. Schalley and P. B. Armentrout, Top. Curr. Chem. **225**, 233–266 (2003).
[38]P. B. Armentrout, J. Chem. Phys. **126**(23), 234302 (2007).
[39]S. E. Wheeler, A. Moran, S. N. Pieniazek, and K. Houk, J. Phys. Chem. A **113**(38), 10376–10384 (2009).
[40]G. P. Wood, L. Radom, G. A. Petersson, E. C. Barnes, M. J. Frisch, and J. A. Montgomery, Jr., J. Chem. Phys. **125**(9), 094106 (2006).
[41]G. A. Petersson, A. Bennett, T. G. Tensfeldt, M. A. Al-Laham, W. A. Shirley, and J. Mantzaris, J. Chem. Phys. **89**(4), 2193–2218 (1988).
[42]G. A. Petersson and M. A. Al-Laham, J. Chem. Phys. **94**(9), 6081–6090 (1991).
[43]L. A. Curtiss, K. Raghavachari, P. C. Redfern, V. Rassolov, and J. A. Pople, J. Chem. Phys. **109**(18), 7764–7776 (1998).
[44]L. A. Curtiss, P. C. Redfern, and K. Raghavachari, J. Chem. Phys. **123**(12), 124107 (2005).
[45]L. A. Curtiss, P. C. Redfern, and K. Raghavachari, J. Chem. Phys. **126**(8), 084108 (2007).
[46]I. M. Alecu, J. Zheng, Y. Zhao, and D. G. Truhlar, J. Chem. Theory Comput. **6**(9), 2872–2887 (2010).
[47]C. Peng and H. B. Schlegel, Isr. J. Chem. **33**(4), 449–454 (1993).
[48]P. B. Armentrout, Int. J. Mass Spectrom. **200**(1), 219–241 (2000).
[49]H. Koizumi, M. Larsen, P. B. Armentrout, and D. Feller, J. Phys. Chem. A **107**(16), 2829–2838 (2003).
[50]P. B. Armentrout and E. M. Stennett, J. Am. Soc. Mass Spectrom. **25**(4), 512–523 (2014).
[51]L. A. Angel and K. M. Ervin, J. Phys. Chem. A **108**(40), 8346–8352 (2004).
[52]R. H. Schultz, K. C. Crellin, and P. B. Armentrout, J. Am. Chem. Soc. **113**(23), 8590–8601 (1991).
[53]D. Schröder, H. Schwarz, D. E. Clemmer, Y. Chen, P. B. Armentrout, V. I. Baranov, and D. K. Böhme, Int. J. Mass Spectrom. **161**(1), 175–191 (1997).
[54]Y.-M. Chen and P. B. Armentrout, Chem. Phys. Lett. **210**(1), 123–128 (1993).
[55]R. H. Schultz and P. B. Armentrout, J. Chem. Phys. **96**(2), 1046–1052 (1992).
[56]M. McCarthy, C. Gottlieb, H. Gupta, and P. Thaddeus, Astrophys. J. **652**(2), L141 (2006).
[57]J.-D. Chai and M. Head-Gordon, Phys. Chem. Chem. Phys. **10**(44), 6615–6620 (2008).
[58]J.-D. Chai and M. Head-Gordon, J. Chem. Phys. **128**(8), 084106 (2008).
[59]J. C. Rienstra-Kiracofe, G. S. Tschumper, H. F. Schaefer, S. Nandi, and G. B. Ellison, Chem. Rev. **102**(1), 231–282 (2002).